

**TOWARDS A BOTTOM-UP RECONSTITUTION  
OF THE NUCLEAR PORE COMPLEX**



# **TOWARDS A BOTTOM-UP RECONSTITUTION OF THE NUCLEAR PORE COMPLEX**

## **Dissertation**

for the purpose of obtaining the degree of doctor  
at Delft University of Technology,  
by the authority of the Rector Magnificus, Prof.dr.ir. T.H.J.J. van der Hagen,  
chair of the Board for Doctorates to be defended publicly on  
Friday 12th November 2021 at 15:00 o' clock

by

**Alessio FRAGASSO**

Master of Science in Nanotechnologies for ICTs,  
Politecnico di Torino, Grenoble INP Phelma, and École  
Polytechnique Fédérale de Lausanne,  
born in Camposampiero, Italy.

This dissertation has been approved by the  
promotor: Prof. dr. C. Dekker

Composition of the doctoral committee:

Rector Magnificus	chairperson
Prof. dr. C. Dekker	Delft University of Technology

*Independent members:*

Prof. dr. M. Dogterom	Delft University of Technology
Prof. dr. R. Lim	University of Basel
Prof. dr. A. Zilman	University of Toronto
Prof. dr. L. M. Veenhoff	University of Groningen
Dr. S. Caneva	Delft University of Technology
Prof. dr. B. Rieger	Delft University of Technology, reserve member

*Other members:*

Prof. dr. P. R. Onck	University of Groningen
----------------------	-------------------------



*Keywords:* nuclear pore complex; nanopores; FG nups; intrinsically disordered proteins; biomimetics; DNA origami; 1/f noise

*Printed by:* Gildeprint

*Front & Back:* Erik Major

Copyright © 2021 by A. Fragasso

Casimir PhD Series, Delft-Leiden 2021-28

ISBN 978.90.8593.494.3

An electronic version of this dissertation is available at  
<http://repository.tudelft.nl/>.

# CONTENTS

<b>1 General Introduction</b>	<b>1</b>
1.1 Introduction . . . . .	2
1.2 The nuclear pore complex . . . . .	3
1.3 Bottom-up approaches to unravel the NPC . . . . .	7
1.4 Single-molecule sensing with nanopores . . . . .	7
1.5 DNA origami nanotechnology . . . . .	10
1.6 In this thesis . . . . .	12
References . . . . .	14
<b>Summary</b>	<b>21</b>
<b>Samenvatting</b>	<b>25</b>



# 1

## GENERAL INTRODUCTION

*In this chapter I present a general introduction to the thesis. While the main interest is to understand the mechanism by which the nuclear pores in our cells operate, various topics and techniques are touched upon. Starting from a brief overview of the cellular organization, I narrow down into the nuclear pore complex, from the first discoveries of its architecture and composition to recent theories describing how nuclear transport is regulated. Furthermore, I discuss the importance of biomimetic approaches to study nuclear transport, with a particular emphasis on solid-state-nanopore and DNA-origami technologies.*

## 1

## 1.1. INTRODUCTION

Life on earth is extremely diverse and variegated, from single-cell entities like bacteria or yeast, to complex multi-tissue organisms such as humans. To achieve the sophistication found in more complex systems like eukaryotes, molecules are organized into organelles which, just like the organs in our body, carry out different specialized tasks (Figure 1.1a) [1]. For example, mitochondria produce the chemical energy needed to perform biochemical reactions in the cell, ribosomes read strings of mRNA to synthesize new proteins, while the nucleus stores the hereditary information in the form of DNA[2]. To safely protect the genetic material, eukaryotic cells feature a double membrane nuclear envelope (NE) that encloses and physically isolates the nucleus from the rest of the cell [3].

Nuclear Pore Complexes (NPCs) are large protein assemblies that form ~40nm-wide channels across the NE and behave as gatekeepers by controlling the trafficking of RNAs, proteins, and metabolites between the nucleus and the cytoplasm (Fig.1.1b) [4]. In a single cell, the number of nuclear pores can vary from 75–150 in a yeast cell [5] to ~3000–5000 pores in a human cell [6], to  $\sim 5 \times 10^7$  in a mature *Xenopus* oocyte [7]. A fascinating aspect of the NPC is its unique combination of high versatility while retaining specificity. In fact, up to 30 different types of transporter proteins are recognized and allowed to efficiently translocate through the NPC, while precluding the transport to all other large molecules [8]. The secret for such highly selective transport relies in a group of key proteins, called FG-Nups, which form a tangled spaghetti-like mesh within the central channel of the NPC [9].

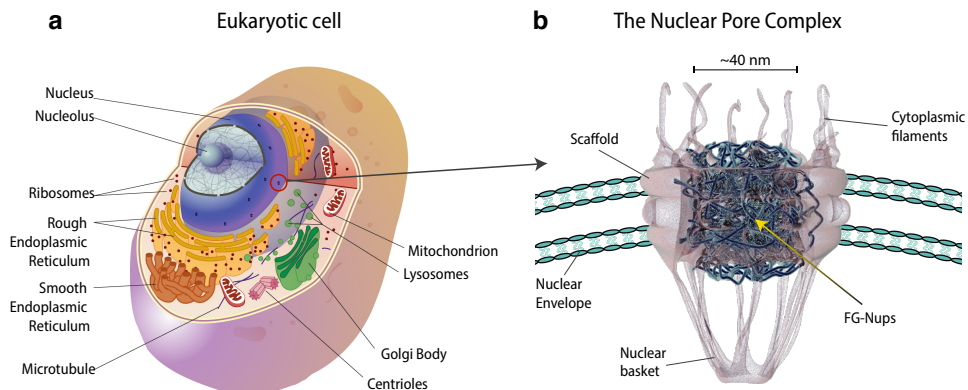


**Figure 1.1:** a, Schematic of an eukaryotic cell, adapted from [10]. b, Illustration of the nuclear pore complex embedded in the nuclear envelope. FG-Nups (blue) line the central channel forming a spaghetti-like mesh. Adapted from a design of Samir Patel.

In this thesis, we work towards understanding the physical principles underlying this remarkable NPC selectivity, leveraging on techniques from molecular biology to nanotechnology. To understand and properly interpret the signal coming from our nanodevices, we first delve into a physical characterization of the noise sources that affect ion current measurements in solid-state nanopores. We then move on to engineer a fully

synthetic FG-Nup from scratch and study its selective properties by reconstituting an artificial mimic of the NPC transport barrier using such a designer protein. Additionally, we provide supporting evidence that point to a mechanistic description of nuclear transport by studying the behavior of a purified native FG-Nup. Finally, we take a major step towards the reconstitution of an artificial nucleus by embedding 30nm-wide DNA-origami pores into the membrane of a lipid vesicle. The present work opens the way to multiple exciting applications and follow-up projects towards the recapitulation and physical understanding of nuclear transport, as well as creating artificial models of the nucleus that can be employed in synthetic cells.

## 1.2. THE NUCLEAR PORE COMPLEX

### 1.2.1. ARCHITECTURE AND COMPOSITION

First evidence of the existence of the NE and nuclear pores was provided in 1950 by Callan and Tomlin [11], who performed imaging of the nuclear membrane of oocytes from amphibia using electron microscopy (EM). Further investigation by Gall in 1967 [12] revealed the octagonal symmetry of nuclear pores (Figure 1.2a,b), which was confirmed by other follow-up studies [13, 14]. Further refinements of the NPC structure using EM allowed to resolve other peripheral parts of the NPC, which include the cytoplasmic filaments and nuclear basket (Fig.1.2c–e, [refs]) [15, 16]. The biochemical composition of the NPC consists of ~30 different types of nucleoporins (Nups) repeated in multiple copies following the octagonal symmetry of the pore. The distribution of Nups is modular and they can be distinguished in three categories [17, 18]: (1) transmembrane Nups that anchor the NPC to the NE; (2) scaffold Nups that form a rigid ring-like

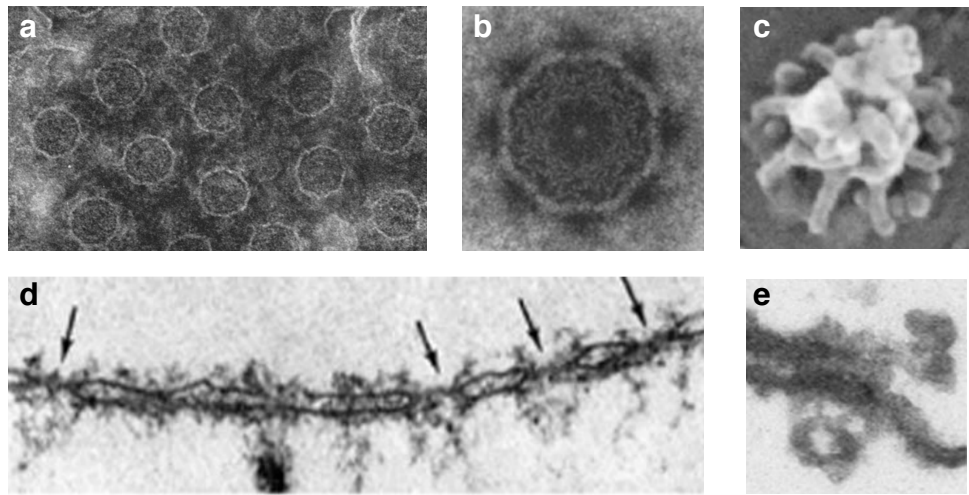


**Figure 1.2:** a,b, Negative staining EM showing octagonal cross-sections of nuclear pore complexes extracted from *Triturus alpestris* nuclei (adapted from [12]). c, Electron microscopy structure of the nuclear pore complex from the nucleoplasmic side. Adapted from [15]. d, Negative staining EM of the nuclear envelope featuring embedded NPCs (pointed by arrows). Adapted from [16]). e, Transmission electron microscopy image of a nuclear pore complex. Adapted from [19].

structure to which intrinsically disordered (3) FG-Nups, rich in tandem ‘Phenylalanine-Glycine’ (FG) repeats, are anchored by their C-terminal domain and fill up the NPC central channel forming a gel-like mesh.

### 1.2.2. FG-NUPS – TYPES AND MOTIFS

The central channel of the NPC is lined with intrinsically disordered FG-Nups (11 different types in yeast [20]). Based on their amino-acid sequence, FG-Nups appear quite redundant, with all of them featuring tandem Phe-Gly (FG) repeats separated by spacer sequences of ~5-20 amino-acids (Fig.1.3a) [21]. Moreover, they are evolutionary conserved in their overall composition and structure [22]. FG-Nups can be broadly divided into two main categories [20, 21]: (1) FXFG-Nups which are abundant in Phe-Any-Phe-Gly (FXFG) repeats, where ‘X’ can be any amino-acid, featuring spacers relatively high in charge (~26-36% of amino-acids has a charge), which confer FXFG-Nups with an overall extended and dynamic conformation; (2) GLFG-Nups that instead are rich in Gly-Leu-Phe-Gly (GLFG) repeats with spacer sequences enriched in ‘Q’ and ‘N’ amino-acids. Unlike FXFG-Nups, these possess a low amount of charged amino-acids (2-3%) resulting in a more collapsed coil configuration. Strikingly, deletion of all FG-Nups other than the GLFG-Nups Nup100, Nup116, and Nup145, was shown to still support efficient nuclear transport *in vivo* without impairing the viability of the cell, which showcases the outstanding robustness and redundancy of the FG-Nup barrier [24].

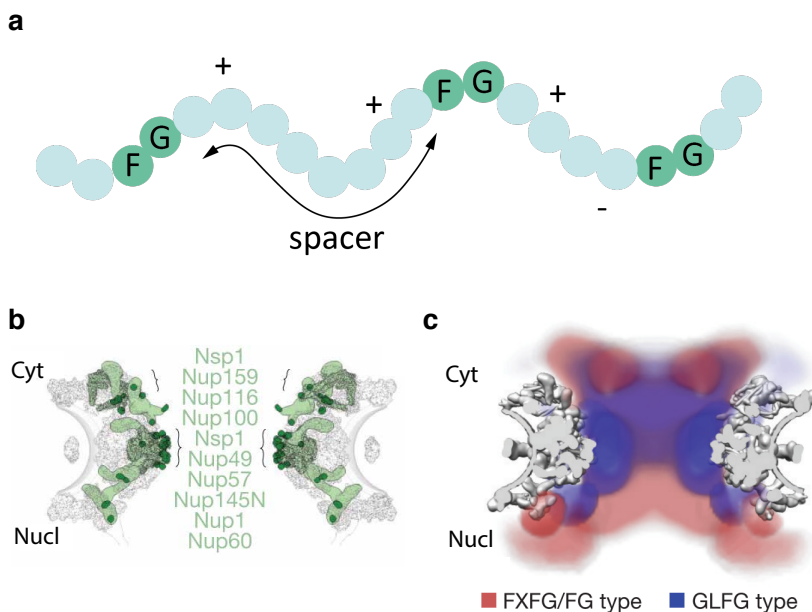


**Figure 1.3:** a, Representation of a characteristic FG-Nup protein sequence. b, Structure of the NPC scaffold (grey) with highlighted FG-Nups anchor domains (light green) and FG-repeat emanating points (dark green). c, Heat map of the GLFG (purple) and FXFG (red) domains from Brownian dynamics simulations. b and c were adapted from [23].

### 1.2.3. NUCLEOCYTOPLASMIC TRANSPORT

FG-Nups are key players in regulating molecular transport across the NE [9]. While allowing the passive diffusion of small molecules, *e.g.* water, ions, and proteins up to a size cut-off of ~40 kDa, transport of large molecules (>40 kDa) occurs selectively [25]: inert macromolecules are hindered by the FG-mesh unless they are bound to a nuclear transport receptor (NTR). Karyopherins (or Kaps) constitute the largest family of NTRs [26], with importin- $\beta$  (Imp $\beta$ , Kap95 in yeast) being the most characterized as it plays a central role in nuclear import [27]. It features ~9-10 hydrophobic pockets on its convex surface that can specifically bind FG-motifs [28], which in turn facilitates its partitioning into the NPC channel. In this way, cargoes that feature a nuclear localization signal (NLS) sequence can form a complex with a NTR and be ferried across the NPC within a few milliseconds (~5 ms [29]).

While maintenance of an efficient and selective transport by the FG-mesh comes at no energy cost, energy is spent in form of GTP hydrolysis to enforce transport directionality of cargoes [30, 31]. For nuclear import (Fig.1.4) of cargo from the cytoplasm into the nucleus, cargo-bound NTRs bind to the nuclear factor RanGTP which induces a NTR conformational change that causes the release of the cargo into the nucleus. The NTR-RanGTP complex is subsequently recycled back into the cytoplasm, where RanGTP is hydrolyzed into RanGDP by the cytoplasmic factor RanGAP1. Such release of energy induces a conformational change that causes the dissociation of the RanGDP-NTR complex, making the NTR available for a new import cycle. RanGDP is then transported back into the nucleus by the transport factor NTF2, where it finally gets converted back into RanGTP by RanGEF. Nuclear export occurs in an analogous way to the import [33].

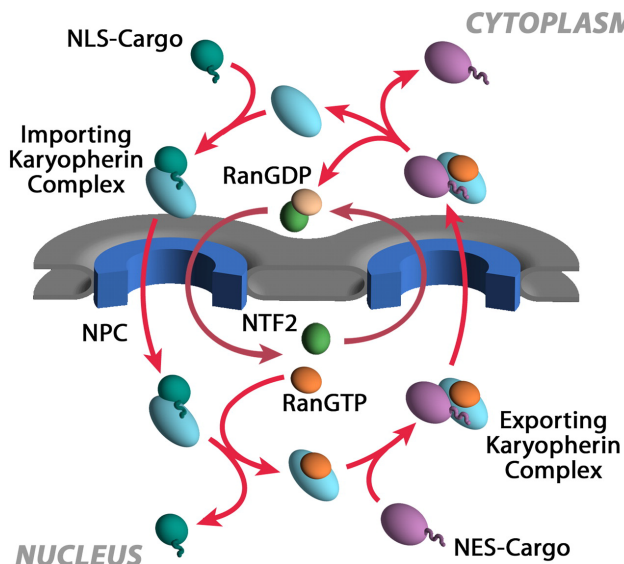


**Figure 1.4:** Schematic of the RanGTP-regulated nuclear transport and their cargoes. Adapted from [32].

## 1

### 1.2.4. MODELS OF SELECTIVE TRANSPORT

While nucleocytoplasmic transport is well characterized in terms of key players and regulation processes, the exact mechanism governing the selective transportation of cargo-bound NTRs through the NPC channel is still disputed. In fact, a number of models have been proposed which can be broadly classified into two opposing theories, termed 'FG-centric' and 'Kap-centric' models:

**FG-centric models:** The first class of models includes the 'virtual gate model' [36], 'selective-phase' or 'hydrogel model' [37, 38], and 'forest model' [20], which predict that FG-Nups are the sole necessary ingredient in establishing the selective barrier. As a corollary, this implies that Kaps act as mere transporters of cargo molecules, without in any way altering the structure of the FG-mesh or taking part into forming the selective barrier (Fig.1.5, left).

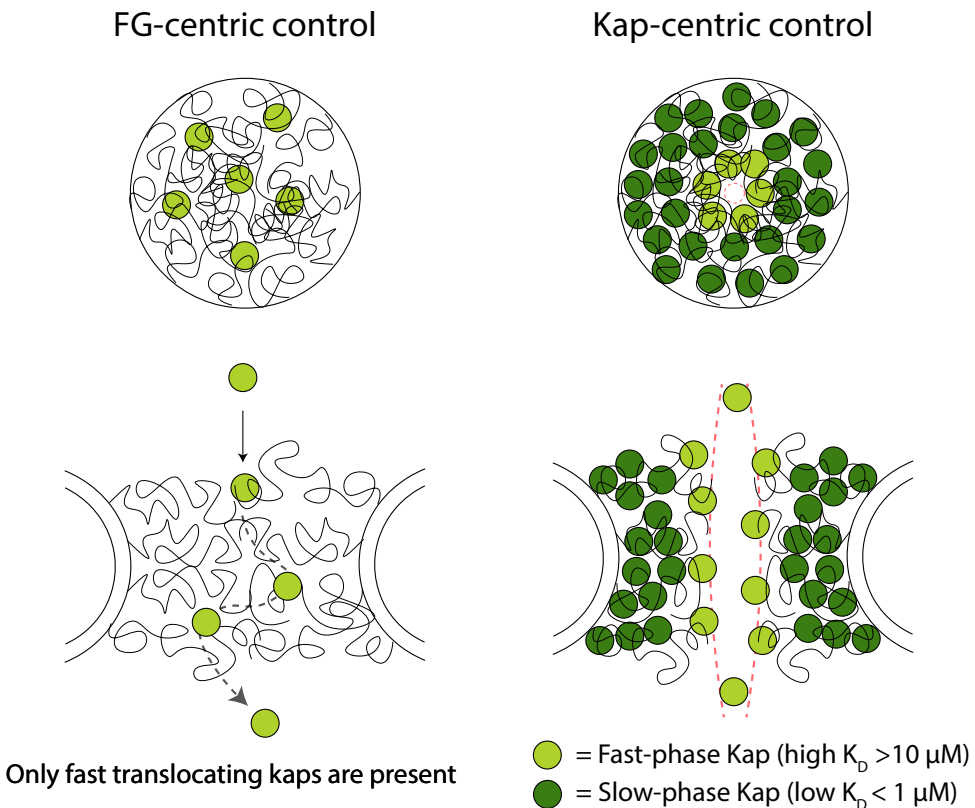


**Figure 1.5:** Simplified schematic of 'FG-centric' (left) and 'Kap-centric' (right) transport. Black curved lines represent FG-Nups, light and dark green circles correspond to the fast-phase and slow-phase Kap population, respectively, dashed black arrow (left) represent a Kap trajectory, dashed red lines (right) indicate the central channel opening. Inspired by [34] and [35].

**Kap-centric models:** The second class of models, such as the ‘reduction of dimensionality model’ [39], ‘molecular velcro model’ [40], and further refinements [34, 35, 41–43], supports the existence of two distinct populations of Kaps – a ‘slow-phase’ and a ‘fast-phase’, where the slow-phase Kaps are involved in reshaping the FG-mesh while opening a central channel by means of avid multivalent binding to FG-repeats, whereas fast-phase Kaps are the actual transporters that shuttle the cargo across the NPC (Fig.1.5, right). Importantly, occupation of the FG-mesh by the slow-phase Kaps would result in a partial depletion of the available FG-repeats hence lowering the affinity between the Kap-laden FG-mesh and the fast-phase Kaps.

### 1.3. BOTTOM-UP APPROACHES TO UNRAVEL THE NPC

Studying transport through the nuclear pore complex *in vivo* still faces significant challenges and limitations due to a lack of spatiotemporal resolution. The NPC is a complex machine, comprising ~200 intrinsically disordered FG-Nups confined into a ~40nm-wide central lumen, with ~1000 molecules per second being transported across in both directions [44]. Gaining mechanistic information on the translocation process of Kap-cargo complexes through the FG-mesh has thus far remained prohibitively difficult.

To overcome such challenges, biomimetic techniques have emerged as an alternative approach to study nuclear transport, where the FG-mesh that is found in the central channel of the NPC is reconstituted *in vitro* and characterized using a variety of tools. Notable examples include surface techniques, such as ellipsometry and QCM-D [45, 46], SPR [34, 47], and AFM force spectroscopy [40, 48], which contributed greatly to the characterization of the binding affinity between Kaps and FG-Nup brushes, where such brushes were formed by anchoring FG-Nups to a planar surface with a grafting density comparable to the one found in the real NPC. Importantly, such techniques revealed the presence of distinct binding modes between Kaps and FG-Nup brushes that vary as a function of Kap concentration and that stem from the multivalent nature of the interaction.

While studying the affinity between transporters and FG-Nups is beneficial and insightful, selective transmembrane transport is arguably the most crucial, yet puzzling, feature of the NPC. To study such important aspect, in the last decade NPC mimics based on artificial nanopores have been built by tethering purified FG-Nups to the inner walls of a nanopore [49, 50]. The appeal of this approach resides in the possibility to reconstitute the selective FG-Nup barrier into a confined nanopore system with virtually the same geometry and FG-Nup density as the NPC central channel. We will now introduce two major realizations of biomimetic nanopores that take advantage of state-of-the-art solid-state and DNA-origami nanotechnology.

### 1.4. SINGLE-MOLECULE SENSING WITH NANOPORES

Advancements in nanotechnology have enabled the fabrication and development of solid-state nanopores [51, 52]. In simple terms, a solid-state nanopore can be described as a nanometer-sized hole formed across a thin (typically ~20 nm) freestanding membrane built from a solid-state material. Over the years, a variety of membranes have been employed as substrates for nanopore fabrication, from the more common low stress sili-

con nitride [53, 54] ( $\text{SiN}_x$ ) to silicon dioxide ( $\text{SiO}_2$ ), as well as ultrathin 2D-materials such as graphene [55, 56], hexagonal boron nitride (hBN) [57, 58], or molybdenum disulfide ( $\text{MoS}_2$ ) [59]. To create such nanoholes various techniques have been developed that respond to different needs in terms of precision, cost, and throughput. To create pores with nanometer-precision a transmission electron microscope (TEM) is usually the preferred choice (Fig. 1.6a,b), where a beam of electrons is focused onto a freestanding membrane which results in removal of atoms from the material and the formation of a hole [60]. A more high-throughput, though less precise, method to fabricate pores is milling using a focused ion beam (FIB) [61, 62], which works analogously to the TEM but with ions (typically  $\text{Ga}^+$  or  $\text{He}^+$ ) instead of electrons. Other techniques are dielectric breakdown [63, 64], laser etching [65], reactive ion etching (RIE) [66], and mechanical pulling of glass capillaries [67].

The most common application of nanopore technology consists in single-molecule sensing, which is achieved by encasing the nanopore chip in a flow cell where the nanopore constitutes the sole connection between two otherwise insulated compartments [68]. Such compartments are filled with a saline aqueous solution, *e.g.* potassium chloride (KCl), which results in free  $\text{K}^+$  and  $\text{Cl}^-$  ions. Application of a voltage difference across the freestanding membrane results in an electric field across the pore that drives positive ions  $\text{K}^+$  to the side with negative potential and  $\text{Cl}^-$  to the positive one. Such flow of ions across the pore results in an ionic current which can be sensed by the electronics and that serves as the signal to perform sensing [69].

The basic principle of nanopore sensing is illustrated in Figure 1.6c,d, where the analyte of interest, such as a protein or a DNA molecule, is electrophoretically driven across the pore by the applied voltage difference which causes the flow of ions to be temporarily interrupted due to the presence of the molecule. This effectively results in a transient, detectable decrease of the ionic current (Fig. 1.6d). Single-molecule translocation events are associated with such current ‘spikes’ and are typically characterized in terms of amplitude (or blockade), namely the depth of the current decrease which is roughly propor-

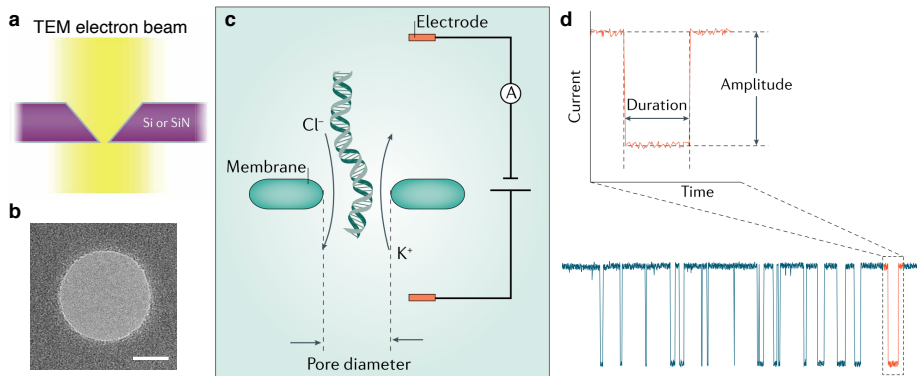


**Figure 1.6:** a, Illustration of nanopore fabrication by TEM drilling. b, TEM micrograph of a nanopore. Scale bar, 30nm. c-d Principle of nanopore sensing: molecules are electrically driven through the pore by an applied potential difference causing transient dips (d) in the ionic current. a, c, d, were adapted from [52].

tional to the size of the analyte, and dwell time which corresponds to the duration of the event and, to a first approximation, reflects how much time the molecule spends in the pore.

### 1.4.1. BIOMIMETIC SOLID-STATE NANOPORES

While nanopores are usually thought of as next-generation sequencers of DNA [70] and proteins [71], an exciting application consists in mimicking biological processes by recapitulating the behavior of naturally occurring pores such as the NPC. In the context of this thesis, a biomimetic solid-state nanopore consists of a solid-state nanopore that is functionalized with FG-nucleoporins from the nuclear pore complex with the aim to mimic as closely as possible the native FG-mesh in terms of spatial confinement, geometry, and protein density, while being able to probe the transport across the pore with single-molecule resolution by measuring the ionic current (Fig.1.7a). Functionalization of the nanopore surface is generally carried out by a chemical conjugation protocol [50, 72], which ensures proper covalent attachment of the proteins to the solid-state material. To test the selective properties of the reconstituted FG-mesh, transporter proteins, such as Imp $\beta$ , are used as positive control since they are naturally capable of interacting with and overcoming the FG-Nup barrier. On the contrary, inert proteins like BSA that lack binding sites for FG-repeats are repelled by the FG-mesh and thereby fail to traverse the pore.

Current measurements are carried out similarly as in a standard nanopore experiment, where the current flowing across the FG-Nup-coated pore reports in real-time on the passage of proteins (Fig1.7b), and thus allows to assess the selective transport properties in terms of event rate, *i.e.* number of translocations per second, which is a measure of the transport efficiency of the analyte across the pore. Notably, such current measurements revealed that biomimetic pores built using a single type of FG-Nup (*e.g.*, Nup98 or Nup153) were enough to impart a selective barrier, where Imp $\beta$  can efficiently translocate while BSA is blocked (Fig.1.7c) [49, 50, 72].

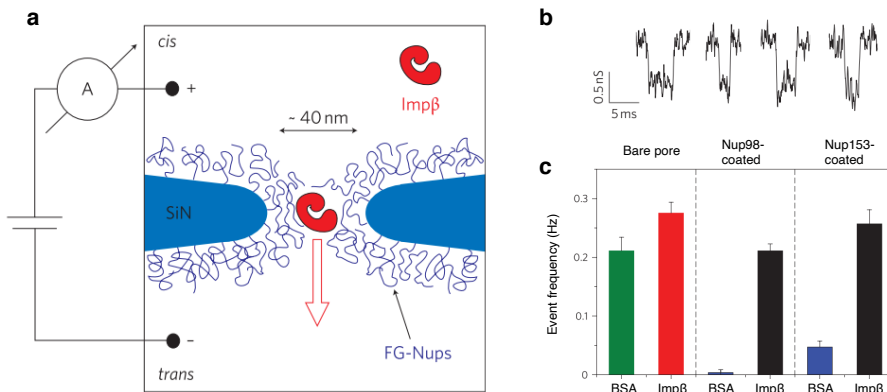


**Figure 1.7:** a, Schematic of a biomimetic solid-state nanopore system. b, Examples of translocation events of Imp $\beta$  through a FG-Nup coated pore. c, Event rate of translocations of BSA and Imp $\beta$  through a bare (left), Nup98-coated (center), and Nup153-coated (right) pores. Adapted from [50].

## 1.5. DNA ORIGAMI NANOTECHNOLOGY

While DNA (deoxyribonucleic acid) in biology assumes the passive role of mere information carrier, as unlike proteins it does not perform any sensory or actuator function in the cell, in the last three decades scientists have been able to use DNA molecules to build 3D nanostructures from scratch in a fully programmable way [73, 74]. Such promising technology, known as ‘DNA origami’, exploits the structure of the DNA molecule that consists of two strands of nitrogenous bases (adenine (A), guanine (G), thymine (T), and cytosine (C)) that are mutually held together by hydrogen bonds resulting in a double helix, where such bonds can occur only between complementary bases A-T and G-C.

Creation of DNA nanostructures relies on using a long single strand of DNA as a scaffold which, upon adding many short DNA strands that staple different parts of the scaffold, is folded into a 3D shape (Fig 1.8a) [75]. Using this relatively simple concept it has been possible to build a multitude of nanostructure for various purposes, from regular shapes such as 2D-sheets and cubes (Fig.1.8b) [73], to more complex structures such as spirals and rings (Fig.1.8c) [76].

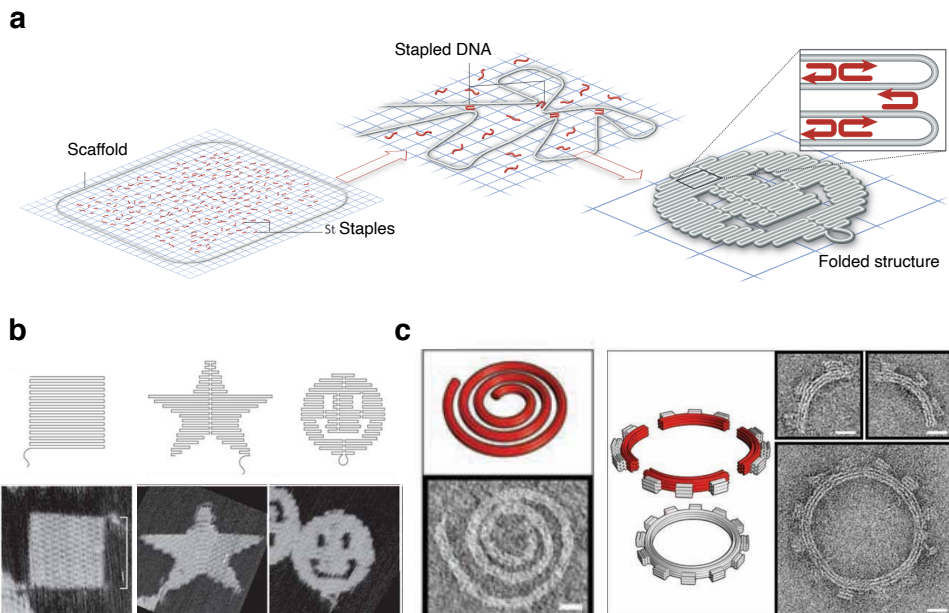


**Figure 1.8:** a, Illustration of the typical DNA origami workflow. A long scaffold of DNA is stapled together by short pieces of DNA to form a stably folded structure. Adapted from [75]. b, Examples of design (top) and AFM images (bottom) of simple DNA-origami structures. Adapted from [73]. c, Examples of complex twisted DNA-origami structures. Scale bars, 20nm. Adapted from [76].

### 1.5.1. DNA ORIGAMI NANOPORES AND NPC MIMICS

A relevant application in the context of this thesis is the construction of DNA-origami pores that mimic the pore-forming properties of naturally occurring protein pores such as  $\alpha$ -hemolysin [77]. Similarly to a biological pore, DNA-origami pores from the literature have been engineered with hydrophobic moieties, such as cholesterol or porphyrins, that aid in the insertion of the highly hydrophilic DNA-object into a lipid bilayer membrane (Fig.1.9) [78]. Using this approach, pores with inner diameters from a few nanometers [79, 80] up to 10 nm [81, 82] have been constructed and shown to spontaneously insert into a lipid membrane by allowing the transmembrane transport of ions [79, 83], fluorophores [81, 84], and short artificial polymers such as PEG [80] and dextran [81, 82].

An exciting feature of DNA-origami pores is the possibility to functionalize the inner walls of the pore to build a mimic of the NPC where FG-Nups distribution and density of the anchor points can be programmed by design. Using this approach, it has been possible to reconstitute NPC mimics by folding DNA-origami rings of ~35-40 nm in inner diameter (similar to the native NPC) and by attaching FG-Nups to their inner surface [85, 86]. However, one major limitation of this approach is the impossibility to measure transport across the reconstituted FG-mesh, since it is extremely challenging to insert such large DNA-objects into a lipid bilayer.

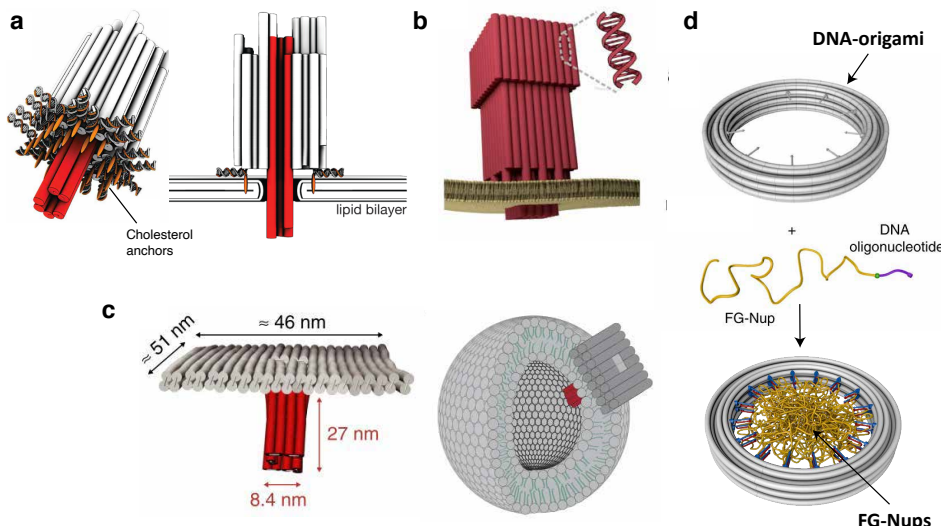


**Figure 1.9:** a, First reported DNA-origami pore with a inner diameter of 2 nm, functionalized with 26 cholesterol anchors (orange). Adapted from [79]. b, Funnel-shaped transmembrane DNA-pore with 6 nm inner diameter. Adapted from [83]. c, T-shaped DNA-origami pore with ~4 nm inner diameter. Adapted from [84]. d, DNA-origami ring scaffold (grey) for FG-Nup (yellow) attachment. Adapted from [85].

## 1.6. IN THIS THESIS

This thesis aims to contribute with novel bottom-up approaches to the field of nuclear transport using biomimetic nanopores. We propose a new model system to understand and capture the essence of FG-Nups, as well as alternative strategies to circumvent the current technical difficulties in current biomimetic DNA-origami nanopore systems. The next two chapters following the introduction are focused on characterization of the noise sources in solid-state nanopores. **Chapter 2**, provides a side-by-side comparison of the noise and performance of biological and solid-state pores. First, the physical origin of the noise at different frequencies is provided together with literature studies and measurements on a few exemplary nanopore systems. Second, the performance of the most relevant biological and solid-state nanopores is compared in terms of signal-to-noise ratio (SNR). We find that SiN<sub>x</sub> pores offer the highest SNR of ~37 when measuring free translocations of short DNA homopolymers through the pores. Introducing a slowdown mechanism using a DNA-translocating motor protein on top of a MspA pore was shown to boost the SNR by >160-fold. Finally, we review reported methods from the literature that were shown to lower the noise for various nanopore systems and frequency ranges. In **Chapter 3**, we explore the low-frequency 1/f noise in solid-state nanopores for varying pore diameters and find that the 1/f noise magnitude decreases for increasing diameter of the pore. To capture this behavior, we build a generalized version of the previously proposed Hooge's model for nanopores that includes explicit contributions from access region and pore surface. Additionally, we define different Hooge parameters for bulk and surface 1/f noise, which represent different mechanisms of fluctuations affecting the ionic current. Such model refinement allows for a more accurate characterization of the 1/f noise in solid-state nanopore systems. **Chapter 4** reviews the state-of-the-art in the field of nanopores, with particular emphasis on applications beyond sequencing. These include single-molecule proteomics, biomarker detection by single-molecule liquid biopsy, pore nanoreactors to confine and study the chemistry of single polymers, and biomimetic nanopore-based approaches to study biological questions.

In **Chapter 5** we introduce a novel, fully bottom-up approach to study nuclear transport by designing an artificial protein, termed 'NupX', that mimics and models native FG-Nups. To design such sequence, we proceed by first analyzing the properties of the naturally occurring GLFG-Nups from yeast. We hypothesize that a finite set of properties characteristic of GLFG-Nups is sufficient for recapitulating their selective behavior, namely: (i) regularly spaced FG and GLFG repeats, (ii) a bimodal distribution of amino acids forming a repulsive and a cohesive domain, and (iii) intrinsic disorder of the amino acid sequence. We first assess the affinity between brushes of our designer NupX and transporter Kap95 using QCM-D, finding that Kap95 binds the protein brush in a concentration-dependent manner. On the contrary, flushing the inert protein BSA does not result in any detectable interaction, thereby proving the binding specificity between Kap95 and NupX. Next, we reconstitute NupX in biomimetic nanopores and test its selective properties, finding that while Kap95 can efficiently translocate through the pore resulting in frequent current spikes, BSA is blocked. Our experiments are complemented by molecular dynamics simulations which provide insights into microscopic features of NupX brushes and coated pores. In summary, this work validates our initial

hypothesis that a rationally designed FG-Nup can reconstitute the archetypal selectivity of the nuclear pore complex.

In **Chapter 6** we reconstitute biomimetic solid-state nanopores using a native FG-Nup, Nsp1, and test its transport properties as a function of Kap95 concentration with the aim to provide new evidence that can aid to discriminate between the different models of transport, specifically between ‘FG-centric’ and ‘Kap-centric’ models. Upon titrating Kap95 onto a Nsp1-coated pore we observe a Kap95 concentration-dependent step-wise decrease of the pore conductance, which indicates Kap95 incorporation into the Nsp1-mesh. Additionally, fast Kap translocations are also observed on top of the current decrease at low ( $\sim 100$  nM) Kap concentrations, similarly to previous reports. On the contrary, flushing inert BSA on a Nsp1-coated pore at increasing concentrations did not result in any detectable current decrease, nor fast translocations, confirming that the observed incorporation of Kap95 into the Nsp1-mesh originates from specific protein-protein interactions and not merely as an effect of the applied bias. Next to a decrease in the pore conductance, we also report a decrease of the low-frequency 1/f noise which is consistent with a stiffening of the Nsp1-mesh upon binding of Kap95. Ion current measurements are corroborated with QCM-D data that, similarly, show a concentration-dependent binding and incorporation of Kap95 into the Nsp1 brush. Altogether, our data are consistent with the ‘slow-phase’ and ‘fast-phase’ Kaps notions introduced by the Kap-centric models.

**Chapter 7** provides an alternative approach to solve the current challenges faced by DNA-origami nanopore systems, namely the difficulty of inserting large DNA-origami objects into lipid membranes. To mimic the eight-fold symmetry and geometry of the NPC, we first design an octagonal DNA-origami scaffold with a nominal inner diameter of 35 nm. Next, we chemically decorate its external surface with hydrophobic moieties which are meant to facilitate the partitioning of the DNA-origami structure into the hydrophobic lipid bilayer. We show that, while DNA-pores do not spontaneously insert into pre-formed lipid bilayers, as expected given the large size, it is possible to circumvent this problem by administering the pores during the vesicle formation by employing an inverted-emulsion cDICE technique to produce the vesicles. To assess the correct insertion of the pores, we carry out influx experiments with the fluorescent protein GFP and find that  $\sim 50\%$  of the vesicle population features open pores. We quantify the influx rate by using a FRAP assay and, using a diffusion model to fit the FRAP data, find that up to hundreds of pores can be properly reconstituted into the membrane of a single vesicle. Furthermore, we show that our pores are size-selective, since dextran molecules with sizes up 28 nm can translocate the pores, whereas larger molecules are excluded. In **Chapter 8**, finally, I provide my perspective on future possible directions and key experiments aimed to address some major open questions in the field of nuclear transport.

## 1

**REFERENCES**

- [1] L. H. B. A. Z. SL, and E. Al., *Molecular Cell Biology*, 4th ed. (W. H. Freeman, New York, 2000).
- [2] D. L. Nelson and M. Cox, *Principles of biochemistry* (W.H. Freeman and Company, New York, 2008).
- [3] M. W. Hetzer, *The Nuclear Envelope*, Cold Spring Harbor perspectives in biology **2**, 1 (2010).
- [4] S. R. Wente and M. P. Rout, *The nuclear pore complex and nuclear transport*. Cold Spring Harbor perspectives in biology **2**, 1 (2010).
- [5] M. Winey, D. Yarar, T. H. Giddings, and D. N. Mastronarde, *Nuclear pore complex number and distribution throughout the *Saccharomyces cerevisiae* cell cycle by three-dimensional reconstruction from electron micrographs of nuclear envelopes*, Molecular Biology of the Cell **8**, 2119 (1997).
- [6] D. Görlich and U. Kutay, *Transport between the cell nucleus and the cytoplasm*, **15**, 607 (1999).
- [7] V. C. Cordes, S. Reidenbach, and W. W. Franke, *High content of a nuclear pore complex protein in cytoplasmic annulate lamellae of *Xenopus* oocytes*, European Journal of Cell Biology **68**, 240 (1995).
- [8] M. Mackmull, B. Klaus, I. Heinze, M. Chokkalingam, A. Beyer, R. B. Russell, A. Ori, and M. Beck, *Landscape of nuclear transport receptor cargo specificity*, Molecular Systems Biology **13**, 962 (2017).
- [9] S. R. Wente, *Gatekeepers of the Nucleus*, Science **288**, 1374 (2000).
- [10] <https://www.genome.gov/genetics-glossary/Organelle>.
- [11] H. G. Callan and S. G. Tomlin, *Experimental studies on amphibian oocyte nuclei. I. Investigation of the structure of the nuclear membrane by means of the electron microscope*. Proceedings of the Royal Society of London. Series B, Containing papers of a Biological character. Royal Society (Great Britain) **137**, 367 (1950).
- [12] J. G. Gall, *Octagonal nuclear pores*. The Journal of cell biology **32**, 391 (1967).
- [13] R. P. Aaronson and G. Blobel, *On the attachment of the nuclear pore complex*, The Journal of Cell Biology **62**, 746 (1974).
- [14] W. W. Franke and U. Scheer, *The ultrastructure of the nuclear envelope of amphibian oocytes: a reinvestigation. II. The immature oocyte and dynamic aspects*, Journal of Ultrastructure Research **30**, 317 (1970).
- [15] M. W. Goldberg, J. M. Cronshaw, E. Kiseleva, and T. D. Allen, *Nuclear-pore-complex dynamics and transport in higher eukaryotes*, Protoplasma **209**, 144 (1999).

- [16] N. Pante and U. Aebi, *Molecular dissection of the nuclear pore complex*, Critical Reviews in Biochemistry and Molecular Biology **31**, 153 (1996).
- [17] D. Devos, S. Dokudovskaya, R. Williams, F. Alber, N. Eswar, B. T. Chait, M. P. Rout, and A. Sali, *Simple fold composition and modular architecture of the nuclear pore complex*, Proceedings of the National Academy of Sciences of the United States of America **103**, 2172 (2006).
- [18] E. Onischenko, J. H. Tang, K. R. Andersen, K. E. Knockenhauer, P. Vallotton, C. P. Derrer, A. Kraft, C. F. Mugler, L. Y. Chan, T. U. Schwartz, and K. Weis, *Natively Unfolded FG Repeats Stabilize the Structure of the Nuclear Pore Complex*, Cell **171**, 904 (2017).
- [19] R. Y. Lim, U. Aebi, and B. Fahrenkrog, *Towards reconciling structure and function in the nuclear pore complex*, Histochemistry and Cell Biology **129**, 105 (2008).
- [20] J. Yamada, J. L. Phillips, S. Patel, G. Goldfien, A. Calestagne-Morelli, H. Huang, R. Reza, J. Acheson, V. V. Krishnan, S. Newsam, A. Gopinathan, E. Y. Lau, M. E. Colvin, V. N. Uversky, and M. F. Rexach, *A Bimodal Distribution of Two Distinct Categories of Intrinsically Disordered Structures with Separate Functions in FG Nucleoporins*, Molecular and Cellular Proteomics **9**, 2205 (2010).
- [21] L. J. Terry and S. R. Wente, *Flexible Gates: Dynamic Topologies and Functions for FG Nucleoporins in Nucleocytoplasmic Transport*, Eukaryotic Cell **8**, 1814 (2009).
- [22] M. Peyro, M. Soheilypour, B. L. Lee, and M. R. Mofrad, *Evolutionarily Conserved Sequence Features Regulate the Formation of the FG Network at the Center of the Nuclear Pore Complex*, Scientific Reports **5**, 1 (2015).
- [23] S. J. Kim, J. Fernandez-Martinez, I. Nudelman, Y. Shi, W. Zhang, B. Raveh, T. Herricks, B. D. Slaughter, J. A. Hogan, P. Upla, I. E. Chemmama, R. Pellarin, I. Echeverria, M. Shivaraju, A. S. Chaudhury, J. Wang, R. Williams, J. R. Unruh, C. H. Greenberg, E. Y. Jacobs, Z. Yu, M. J. de la Cruz, R. Mironksa, D. L. Stokes, J. D. Aitchison, M. F. Jarrold, J. L. Gerton, S. J. Ludtke, C. W. Akey, B. T. Chait, A. Sali, and M. P. Rout, *Integrative structure and functional anatomy of a nuclear pore complex*, Nature **555**, 475 (2018).
- [24] R. L. Adams, L. J. Terry, and S. R. Wente, *A Novel *Saccharomyces cerevisiae* FG Nucleoporin Mutant Collection for Use in Nuclear Pore Complex Functional Experiments*, G3: Genes|Genomes|Genetics **6**, 51 (2016).
- [25] A. Zilman, S. Di Talia, B. T. Chait, M. P. Rout, and M. O. Magnasco, *Efficiency, selectivity, and robustness of nucleocytoplasmic transport*, PLoS Computational Biology **3**, 1281 (2007).
- [26] L. C. Tu and S. M. Musser, *Single molecule studies of nucleocytoplasmic transport*, Biochimica et Biophysica Acta - Molecular Cell Research **1813**, 1607 (2011).
- [27] A. Harel and D. J. Forbes, *Importin beta: Conducting a much larger cellular symphony*, Molecular Cell **16**, 319 (2004).

- 1
- [28] R. Bayliss, T. Littlewood, and M. Stewart, *Structural basis for the interaction between FxFG nucleoporin repeats and importin- $\beta$  in nuclear trafficking*, Cell **102**, 99 (2000).
  - [29] T. Dange, D. Grünwald, A. Grünwald, R. Peters, and U. Kubitscheck, *Autonomy and robustness of translocation through the nuclear pore complex: A single-molecule study*, Journal of Cell Biology **183**, 77 (2008).
  - [30] D. Görlich, N. Panté, U. Kutay, U. Aebi, and F. R. Bischoff, *Identification of different roles for RanGDP and RanGTP in nuclear protein import*, EMBO Journal **15**, 5584 (1996).
  - [31] T. Jovanovic-Talismán and A. Zilman, *Protein Transport by the Nuclear Pore Complex: Simple Biophysics of a Complex Biomachine*, Biophysical journal **113**, 6 (2017).
  - [32] J. D. Aitchison and M. P. Rout, *The yeast nuclear pore complex and transport through it*, Genetics **190**, 855 (2012).
  - [33] B. Cautain, R. Hill, N. De Pedro, and W. Link, *Components and regulation of nuclear transport processes*, FEBS Journal **282**, 445 (2015).
  - [34] L. E. Kapinos, R. L. Schoch, R. S. Wagner, K. D. Schleicher, and R. Y. Lim, *Karyopherin-centric control of nuclear pores based on molecular occupancy and kinetic analysis of multivalent binding with FG nucleoporins*, Biophysical Journal **106**, 1751 (2014).
  - [35] L. E. Kapinos, B. Huang, C. Rencurel, and R. Y. Lim, *Karyopherins regulate nuclear pore complex barrier and transport function*, Journal of Cell Biology **216**, 3609 (2017).
  - [36] M. P. Rout, J. D. Aitchison, M. O. Magnasco, and B. T. Chait, *Virtual gating and nuclear transport: The hole picture*, Trends in Cell Biology **13**, 622 (2003).
  - [37] S. Frey, *FG-Rich Repeats of Nuclear Pore Proteins with Hydrogel-Like Properties*, Science (New York, N.Y.) **314**, 815 (2006).
  - [38] S. Frey and D. Görlich, *A Saturated FG-Repeat Hydrogel Can Reproduce the Permeability Properties of Nuclear Pore Complexes*, Cell **130**, 512 (2007).
  - [39] R. Peters, *Translocation through the nuclear pore complex: Selectivity and speed by reduction-of-dimensionality*, Traffic **6**, 421 (2005).
  - [40] K. D. Schleicher, S. L. Dettmer, L. E. Kapinos, S. Pagliara, U. F. Keyser, S. Jeney, and R. Y. Lim, *Selective transport control on molecular velcro made from intrinsically disordered proteins*, Nature Nanotechnology **9**, 525 (2014).
  - [41] R. Y. Lim and L. E. Kapinos, *How to operate a nuclear pore complex by kap-centric control*, Nucleus **6**, 366 (2015).
  - [42] R. S. Wagner, L. E. Kapinos, N. J. Marshall, M. Stewart, and R. Y. Lim, *Promiscuous binding of karyopherin $\beta$ 1 modulates FG nucleoporin barrier function and expedites NTF2 transport kinetics*, Biophysical Journal **108**, 918 (2015).

- [43] S. Barbato\*, L. E. Kapinos\*, C. Rencurel, and R. Y. Lim, *Karyopherin enrichment at the nuclear pore complex attenuates Ran permeability*, Journal of Cell Science (2020).
- [44] T. Jamali, Y. Jamali, M. Mehrbod, and M. R. Mofrad, *International Review of Cell and Molecular Biology*, 1st ed., Vol. 287 (Elsevier Inc., 2011) pp. 233–286.
- [45] N. B. Eisele, S. Frey, J. Piehler, D. Görlich, and R. P. Richter, *Ultrathin nucleoporin phenylalanine-glycine repeat films and their interaction with nuclear transport receptors*, EMBO Reports **11**, 366 (2010).
- [46] N. B. Eisele, A. A. Labokha, S. Frey, D. Görlich, and R. P. Richter, *Cohesiveness tunes assembly and morphology of FG nucleoporin domain meshworks - Implications for nuclear pore permeability*, Biophysical Journal **105**, 1860 (2013).
- [47] R. L. Schoch, L. E. Kapinos, and R. Y. Lim, *Nuclear transport receptor binding avidity triggers a self-healing collapse transition in FG-nucleoporin molecular brushes*, Proceedings of the National Academy of Sciences of the United States of America **109**, 16911 (2012).
- [48] R. Y. H. Lim, B. Fahrenkrog, J. Köser, K. Schwarz-Herion, J. Deng, and U. Aebi, *Nanomechanical basis of selective gating by the nuclear pore complex*, Science **318**, 640 (2007).
- [49] T. Jovanovic-Talisman, J. Tetenbaum-Novatt, A. S. McKenney, A. Zilman, R. Peters, M. P. Rout, and B. T. Chait, *Artificial nanopores that mimic the transport selectivity of the nuclear pore complex*, Nature **457**, 1023 (2009).
- [50] S. W. Kowalczyk, L. Kapinos, T. R. Blosser, T. Magalhães, P. van Nies, R. Y. H. Lim, and C. Dekker, *Single-molecule transport across an individual biomimetic nuclear pore complex*, Nature Nanotechnology **6**, 433 (2011).
- [51] C. Dekker, *Solid-state nanopores (Review Article)*, Nature Nanotechnology , 1 (2007).
- [52] L. Xue, H. Yamazaki, R. Ren, M. Wanunu, A. P. Ivanov, and J. B. Edel, *Solid-state nanopore sensors*, Nature Reviews Materials (2020), 10.1038/s41578-020-0229-6.
- [53] A. Balan, B. Machielse, D. Niedzwiecki, J. Lin, P. Ong, R. Engelke, K. L. Shepard, and M. Drndić, *Improving signal-to-noise performance for DNA translocation in solid-state nanopores at MHz bandwidths*, Nano Letters **14**, 7215 (2014).
- [54] K. Venta, G. Shemer, M. Puster, J. A. Rodríguez-Manzo, A. Balan, J. K. Rosenstein, K. Shepard, and M. Drndić, *Differentiation of short, single-stranded DNA homopolymers in solid-state nanopores*, ACS Nano **7**, 4629 (2013).
- [55] C. a. Merchant, K. Healy, M. Wanunu, V. Ray, N. Peterman, J. Bartel, M. D. Fischbein, K. Venta, Z. Luo, a. T. C. Johnson, and M. Drndić, *DNA translocation through graphene nanopores*, Nano Letters **10**, 2915 (2010).

- [56] G. F. Schneider, S. W. Kowalczyk, V. E. Calado, G. Pandraud, H. W. Zandbergen, L. M. Vandersypen, and C. Dekker, *DNA translocation through graphene nanopores*, Nano Letters **10**, 3163 (2010).
- [57] Z. Zhou, Y. Hu, H. Wang, Z. Xu, W. Wang, X. Bai, X. Shan, and X. Lu, *DNA Translocation through hydrophilic nanopore in hexagonal boron nitride*, Scientific Reports **3**, 1 (2013).
- [58] K. B. Park, H. J. Kim, H. M. Kim, S. A. Han, K. H. Lee, S. W. Kim, and K. B. Kim, *Noise and sensitivity characteristics of solid-state nanopores with a boron nitride 2-D membrane on a pyrex substrate*, Nanoscale **8**, 5755 (2016).
- [59] M. Graf, M. Lihter, M. Thakur, V. Georgiou, J. Topolancik, B. R. Ilic, K. Liu, J. Feng, Y. Astier, and A. Radenovic, *Fabrication and practical applications of molybdenum disulfide nanopores*, Nature Protocols **14**, 1130 (2019).
- [60] A. J. Storm, J. H. Chen, X. S. Ling, H. W. Zandbergen, and C. Dekker, *Fabrication of solid-state nanopores with single-nanometre precision*, Nature Materials **2**, 537 (2003).
- [61] Y. H. Lanyon, G. De Marzi, Y. E. Watson, A. J. Quinn, J. P. Gleeson, G. Redmond, and D. W. Arrigan, *Fabrication of nanopore array electrodes by focused ion beam milling*, Analytical Chemistry **79**, 3048 (2007).
- [62] B. Schiedt, L. Auvray, L. Bacri, G. Oukhaled, A. Madouri, E. Bourhis, G. Patriarche, J. Pelta, R. Jede, and J. Gierak, *Direct FIB fabrication and integration of "single nanopore devices" for the manipulation of macromolecules*, Microelectronic Engineering **87**, 1300 (2010).
- [63] H. Kwok, K. Briggs, and V. Tabard-Cossa, *Nanopore fabrication by controlled dielectric breakdown*, PLoS ONE **9** (2014), 10.1371/journal.pone.0092880.
- [64] S. Pud, D. Verschueren, N. Vukovic, C. Plesa, M. P. Jonsson, and C. Dekker, *Self-Aligned Plasmonic Nanopores by Optically Controlled Dielectric Breakdown*, Nano Letters **15**, 7112 (2015).
- [65] T. Gilboa, E. Zvuloni, A. Zrehen, A. H. Squires, and A. Meller, *Automated, Ultra-Fast Laser-Drilling of Nanometer Scale Pores and Nanopore Arrays in Aqueous Solutions*, Advanced Functional Materials **1900642**, 1 (2019).
- [66] D. V. Verschueren, W. Yang, and C. Dekker, *Lithography-based fabrication of nanopore arrays in freestanding SiN and graphene membranes*, **29**, 145302 (2018), arXiv:15334406 .
- [67] J. D. Piper, R. W. Clarke, Y. E. Korchev, L. Ying, and D. Klenerman, *A renewable nanosensor based on a glass nanopipette*, Journal of the American Chemical Society **128**, 16462 (2006).
- [68] G. Maglia, A. J. Heron, D. Stoddart, D. Japrung, and H. Bayley, *Methods in Enzymology*, 1st ed., Vol. 475 (Elsevier Inc., 2010) pp. 591–623, arXiv:NIHMS150003 .

- [69] S. Howorka and Z. Siwy, *Nanopore analytics: Sensing of single molecules*, Chemical Society Reviews **38**, 2360 (2009).
- [70] E. Manrao, T. Z. Butler, M. Pavlenok, M. D. Collins, M. Niederweis, J. H. Gundlach, and I. M. Derrington, *Nanopore DNA sequencing with MspA*, Proceedings of the National Academy of Sciences **107**, 16060 (2010).
- [71] H. Brinkerhoff, A. S. W. Kang, J. Liu, A. Aksimentiev, and C. Dekker, *Infinite re-reading of single proteins at single-amino-acid resolution using nanopore sequencing*, bioRxiv , 2021.07.13.452225 (2021).
- [72] A. N. Ananth, A. Mishra, S. Frey, A. Dwarkasing, R. Versloot, E. van der Giessen, D. Görlich, P. Onck, and C. Dekker, *Spatial structure of disordered proteins dictates conductance and selectivity in nuclear pore complex mimics*, eLife **7**, 1 (2018).
- [73] P. W. Rothemund, *Folding DNA to create nanoscale shapes and patterns*, Nature **440**, 297 (2006), arXiv:0202466 [cond-mat] .
- [74] K. F. Wagenbauer, F. A. Engelhardt, E. Stahl, V. K. Hechtl, P. Stömmer, F. Seebacher, L. Meregalli, P. Ketterer, T. Gerling, and H. Dietz, *How We Make DNA Origami*, ChemBioChem **18**, 1873 (2017).
- [75] K. Sanderson, *What to make with DNA origami*, Nature **464**, 158 (2010).
- [76] H. Dietz, S. M. Douglas, and W. M. Shih, *Folding DNA into twisted and curved nanoscale shapes*, Science **325**, 725 (2009), arXiv:9910002 [quant-ph] .
- [77] T. Sugawara, D. Yamashita, K. Kato, Z. Peng, J. Ueda, J. Kaneko, Y. Kamio, Y. Tanaka, and M. Yao, *Structural basis for pore-forming mechanism of staphylococcal  $\alpha$ -hemolysin*, Toxicon **108**, 226 (2015).
- [78] S. Hernández-Ainsa and U. F. Keyser, *DNA origami nanopores: Developments, challenges and perspectives*, Nanoscale **6**, 14121 (2014).
- [79] T. G. Martin, F. C. Simmel, V. Arnaut, M. Mayer, H. Dietz, M. Langecker, S. Renner, and J. List, *Synthetic Lipid Membrane Channels Formed by Designed DNA Nanostructures*, Science **338**, 932 (2012).
- [80] J. R. Burns, A. Seifert, N. Fertig, and S. Howorka, *A biomimetic DNA-based channel for the ligand-controlled transport of charged molecular cargo across a biological membrane*, Nature Nanotechnology **11**, 152 (2016).
- [81] R. P. Thomsen, M. G. Malle, A. H. Okholm, S. Krishnan, S. S. Bohr, R. S. Sørensen, O. Ries, S. Vogel, F. C. Simmel, N. S. Hatzakis, and J. Kjems, *A large size-selective DNA nanopore with sensing applications*, Nature Communications **10** (2019), 10.1038/s41467-019-13284-1.
- [82] S. Iwabuchi, I. Kawamata, S. Murata, and S.-i. M. Nomura, *Large, square-shaped, DNA origami nanopore with sealing function on giant vesicle membrane*, Chemical Communications (2021), 10.1039/d0cc07412h.

- [83] K. Göpfrich, C.-Y. Li, M. Ricci, S. P. Bhamidimarri, J. Yoo, B. Gyenes, A. Ohmann, M. Winterhalter, A. Aksimentiev, and U. F. Keyser, *Large-Conductance Transmembrane Porin Made from DNA Origami*, ACS Nano **10**, 8207 (2016).
- [84] S. Krishnan, D. Ziegler, V. Arnaut, T. G. Martin, K. Kapsner, K. Henneberg, A. R. Bausch, H. Dietz, and F. C. Simmel, *Molecular transport through large-diameter DNA nanopores*, Nature Communications **7**, 1 (2016).
- [85] P. Ketterer, A. N. Ananth, D. S. Laman Trip, A. Mishra, E. Bertosin, M. Ganji, J. Van Der Torre, P. Onck, H. Dietz, and C. Dekker, *DNA origami scaffold for studying intrinsically disordered proteins of the nuclear pore complex*, Nature Communications **9**, 1 (2018).
- [86] P. D. E. Fisher, Q. Shen, B. Akpinar, L. K. Davis, K. K. H. Chung, D. Baddeley, A. Šarić, T. J. Melia, B. W. Hoogenboom, C. Lin, and C. P. Lusk, *A Programmable DNA Origami Platform for Organizing Intrinsically Disordered Nucleoporins within Nanopore Confinement*, ACS Nano **12**, 1508 (2018).

# SUMMARY

At first glance nanopores may appear simple, almost intuitive, to understand given that they are, quite literally, ‘just’ very small pores in a membrane. In fact, one may even wonder why at all we need trained scientists to study such seemingly simple entities. The short answer is that nanopores, as the word suggests, are nanoscale entities and, as such, one can not directly see or experience any of the events that occur down there. The long answer can be found in this thesis. Here, I present and discuss a wide array of nanopores, from biological nanopores like the nuclear pore complex (NPC), to solid-state nanopores, and DNA-origami nanopores. While the central focus of my research is to understand the inner workings of the NPC, a short journey into the world of ion transport in solid-state nanopores is first undertaken, with special emphasis on the random fluctuations of the ion flow within the nanopore, referred to as current noise. Next, I introduce the concept of biomimetic nanopores, where a solid-state nanopore is ‘camouflaged’ by coating its inner surface with purified proteins, resulting in an entity that behaves somewhat like a real NPC. Biomimetic nanopores have enabled us to mimic, study, and gain new insights into how the real NPC works, and bear great potential for further developments and discoveries.

**Chapter 1** provides a general introduction to the basic concepts used this thesis. Starting from a short overview of the cellular organization, I narrow down to the NPC, from the first discoveries of its architecture and biochemical composition, to the key role of FG-Nups in establishing the selective barrier. The current theories of nuclear transport are also illustrated, with emphasis on the two opposing ‘FG-centric’ and ‘Kap-centric’ models. Our experiments take advantage of many tools from nanotechnology. Therefore, I first introduce the nanopore technology, outlining common techniques of fabrication as well as illustrating the basic principles of single-molecule sensing. Following up, I present how engineered solid-state nanopores with FG-Nups have been shown to recapitulate NPC-like selective transport *in vitro*. I end up by explaining the basic principles behind the DNA origami technique, and highlight important literature contributions to the field of DNA-origami nanopores.

**Chapter 2** features a side-by-side comparison of the noise characteristics and performances of biological *vs* solid-state nanopores. We start by introducing the various types of low- and high-frequency noise sources in the two systems. While they both suffer from the same noise sources at high frequencies, namely dielectric and capacitive noise, at low frequencies solid-state nanopores are largely dominated by 1/f noise, whereas biological pores typically feature protonation noise. We move on to confront the performances of a few selected nanopore systems in terms of signal-to-noise ratio (SNR) for free translocations of short homopolymers. We collected data both from literature, our own lab, as well as external labs, and found that SiN<sub>x</sub> solid-state pores featured the

highest SNR (~37), which results from the combination of higher currents, hence higher signal, and low high-frequency noise that are attainable in such system. We note however that introducing a slow-down mechanism using a DNA-motor protein to feed the DNA molecule into the pore, as it was shown for the biological pore MspA, was shown to boost the SNR by >160-fold. We conclude with an overview of the most notable approaches to lower the noise at low and high frequency, for both biological and solid-state nanopores.

To this date, there is still one noise source that puzzles many nanopore researchers, namely the  $1/f$  noise. In **Chapter 3** we characterize the low-frequency spectrum of our solid-state nanopores and find that the magnitude of the  $1/f$  noise fluctuations decreases for larger pores. While such behavior is interesting and appeared as well in previous works, no theoretical model has yet been able to express such trend analytically. We find that including the access region contribution into the picture, which had been dismissed in previous models, is sufficient to fit the general observed trend. We further adopt two different Hooge parameters for surface and bulk fluctuations, which reflect the presence of two different mechanisms of ion fluctuations occurring near the pore surface and in the pore bulk and access regions, respectively. Our model represents a generalization of the Hooge's model for solid-state nanopores that works well for varying nanopore diameters.

**Chapter 4** provides a general overview of the nanopore field, with particular emphasis on nanopore applications beyond sequencing of DNA or RNA. By listing major contributions to the nanopore field from different areas of expertise, we showcase the high versatility of both biological and solid-state nanopore platforms and their applicability to solve a broad range of challenges. The high versatility of nanopores stems from the possibility to control the pore geometry, such as diameter and length, as well as to engineer the pore surface to tune and customize the interaction with the analyte molecules. In this review chapter, we cover a range of applications that involve both biological and solid-state nanopores, from single-molecule proteomics, single-molecule liquid biopsy for detection of relevant biomarkers, creation of nanoreactors to study polymers in confinement, to biomimetic nanopores to mimic and understand complex biological processes. In this thesis, we employ such biomimetic nanopores to investigate the physical principles of the NPC selective barrier.

Building on previous works that showed the successful reconstitution of biomimetic nuclear pore complexes using purified native FG-Nups and solid-state nanopores, we take a step forward in **Chapter 5** and reconstitute fully artificial biomimetic NPCs in solid-state nanopores using a rationally designed FG-Nup protein that we coined 'NupX'. We hypothesise that building a designer protein following a few simple design rules is sufficient for recapitulating a functional, selective biomimetic NPC. From studying the sequence of native yeast GLFG-Nups, known to be essential for proper nuclear transport and cell viability, we identify three recurring properties: (i) a bimodal distribution of amino acids featuring a N-terminal cohesive, low charge domain, and a C-terminal repulsive, high charge domain; (ii) regularly spaced FG and GLFG repeats in the cohe-

sive domain, at intervals of ~ 5 – 20 amino acid spacers; (iii) intrinsically disordered sequences.

To assess the selective properties of our designed sequence, we reconstitute NupX brushes on QCM-D and monitor binding to increasing concentrations of transporter Kap95, finding that Kap95 binds efficiently to NupX in a concentration-dependent manner, similar to native FG-Nups. Conversely, flushing inert BSA yielded no detectable binding to NupX, indicating that NupX binds selectively to Kap95. Next, we reconstituted NupX in biomimetic nanopores and tested the selective transport properties of the reconstituted NupX-mesh. We find that, while flushing transporter Kap95 results in frequent current spikes that indicates efficient transportation of the protein through the pore, inert BSA is virtually blocked as it yields only few sporadic translocation events. Experimental work is complemented by molecular dynamics simulations that provide microscopic insights into the NupX-brushes conformation and NupX-mesh density distribution within the pore. Altogether, our data show the successful recapitulation of nuclear transport selectivity using a rationally designed protein.

In **Chapter 6** we study the interaction between transporter Kap95 and a native FG-nucleoporin, Nsp1, using biomimetic nanopores. While mere selective properties of the reconstituted Nsp1-mesh have been characterized in earlier studies, we here assess the behavior of the Nsp1-mesh as a function of Kap95 concentration with the aim to provide new evidence that aids in discriminating between the current models of transport. First, we create biomimetic nanopores by grafting Nsp1 proteins to the inner wall of a solid-state nanopore. Upon flushing Kap95 in the bulk solution surrounding the pore, we observe a steady-state decrease of the ionic current, indicating that a portion of Kap95 molecules binds with high affinity to the Nsp1-mesh. Furthermore, fast (~millisecond) conductance blockades are observed on top of the current decrease, indicating the presence of a second population of fast translocating Kap95 molecules. We analyse the low-frequency noise of the ionic current, which in biomimetic nanopores is dominated by the FG-Nup fluctuations within the pore, and find a progressive decrease of the 1/f noise at increasing Kap95 concentration, which is consistent with an increase in overall rigidity of the FG-mesh. We corroborate our electrical measurements with QCM-D, where, similar to previous reports, we observe a concentration-dependent incorporation of Kap95 into the Nsp1 brush, consistent with the nanopore experiments. To sum up, our data support the presence of two distinct Kap populations within the FG-mesh, one slow and one fast, which is consistent with predictions from Kap-centric models of transport.

The search for improved NPC mimics led scientists to develop DNA-origami scaffolds to accommodate and spatially organize FG-Nups in a controlled fashion. While NPC mimics based on DNA origami have been reported, it has not been possible, so far, to assess the transport properties of the reconstituted FG-mesh. In **Chapter 7** we address this important issue and work out a novel method to embed very large 30nm-wide DNA-origami pores across the membrane of giant liposomes. To overcome the high energy barrier for insertion of large objects into the lipid bilayer, we adopt an inverted-emulsion cDICE technique which allows us to incorporate the pores into the vesicle membrane during the process of membrane formation. We assess the correct insertion of the pores

by studying the influx of different fluorescent molecules into the vesicle, finding that a range of molecules can pass through the pore, from the smaller ~30 kDa protein GFP, to large 250 kDa (~28 nm) dextran molecules, whereas larger dextran molecules are excluded, consistently with the pore size cut-off. Furthermore, we quantify the number of pores per vesicle using a FRAP assay and modelling the diffusion of GFP through the pores, finding that up to hundreds of pores can be functionally reconstituted into the membrane of a single vesicle. Altogether, these data show the successful reconstitution of large DNA-origami pores into a lipid bilayer, paving the way to further developments from mimicking nuclear transport to recapitulating an artificial nucleus.

To conclude, in **Chapter 8** we look back at the results provided in this thesis and propose new possible developments and follow-up projects that will further shed light on remaining unresolved issues. We first hypothesize that a simple framework that describes necessary and sufficient requirements for FG-Nup selectivity can be achieved by studying the behavior of designer FG-Nups upon systematic variations of the amino acid sequence. In light of the compelling evidence showing the participation of Karyopherins into establishing the selective barrier, we also point to new possible experiments and expansions of the current techniques to further our understanding of the complex Kap-Nup interaction. Next, we point to possible routes for exploiting the newly developed DNA-origami nanopore platform for studying transport through a potentially more controlled, tunable, and physiologically relevant FG-mesh. To conclude, we zoom out to the broad field of nuclear transport and provide our perspective on remaining outstanding questions. I am confident that tackling the current unresolved issues related to our understanding of FG-Nup phase separation, the interplay with Kaps, and the fuzzy architecture of NPC central channel will ultimately provide a satisfying mechanistic understanding of selective nuclear transport.

# SAMENVATTING

Op het eerste gezicht lijken nanoporiën misschien eenvoudig om te doorgronden, want het zijn (letterlijk) slechts heel kleine gaatjes in een membraan. En u zou zich zelfs kunnen afvragen waarom we überhaupt zoveel hoogopgeleide wetenschappers nodig hebben om zulke eenvoudige objecten te bestuderen. Het korte antwoord is omdat nanoporiën, zoals de naam al doet vermoeden, objecten zijn op de nanometer schaal, die men dus niet zo makkelijk kan zien of anderszins kan waarnemen. Het uitgebreide antwoord kunt u vinden in dit proefschrift, waarin ik mijn onderzoek aan vele verschillende typen van nanoporiën beschrijf en bediscussieer. De typen variëren van biologische nanoporiën tot vaste-stof nanoporiën en DNA-origami nanoporiën. Het centrale thema van mijn onderzoek is echter het moleculaire complex dat zich bevindt in de kernporie (nuclear pore complex, of kortweg 'NPC' in het Engels): de nanoporie in het biologische membraan dat de celkern, met daarin het erfelijk DNA materiaal, scheidt van het cytoplasma. Maar voordat ik daartoe kom zal ik u eerste meenemen naar de wonderre wereld van ionen die door vaste-stof nanoporiën stromen en de fluctuaties die zich daarvan voordoen, beter bekend als stroomruis. Vervolgens komen we aan bij het concept van de biomimetische nanoporiën, oftewel vaste-stof nanoporiën die we in het laboratorium zo veel mogelijk laten lijken op biologische nanoporiën, door ze te bedekken met biologische membranen en/of biologische eiwitten. Hierdoor komt het gedrag van deze biomimetische nanoporiën verbazingwekkend dicht in de buurt van dat van de echte kernporie in de cel. Deze biomimetische nanoporiën stellen ons dus in staat om beter te doorgronden hoe de kernporie van onze cellen zich gedragen, en bieden veel potentie voor nieuwe wetenschappelijke ontdekkingen.

**Hoofdstuk 1** is de algemene inleiding op dit proefschrift, waarin de benodigde natuurkundige basisprincipes aan de orde komen, alsmede een kort overzicht van de opbouw van een biologische cel. Vervolgens zal ik inzoomen op de kernporie, door te beschrijven hoe deze werd ontdekt, hoe ze eruit ziet, en uit welke eiwitten ze is opgebouwd. Ook zal ik uitleggen hoe de zogenaamde FG-Nup eiwitten een cruciale poortwachter-achtige rol vervullen, waardoor alleen een selecte groep van biologische moleculen getransporteerd kan worden door de kernporie. Daarnaast zal ik in dit hoofdstuk de gangbare theorieën aanstippen voor het mechanisme van transport door de kernporie, waarbij de nadruk zal liggen op het 'FG-centrische' model en het conflicterende 'Kap-centrische' model. Omdat wij in onze experimenten veel gebruik maken van nanotechnologie zal ik in dit hoofdstuk ook de methoden en technieken beschrijven waarmee we onze onderzoeksobjecten fabriceren, en hoe we één enkel molecuul kunnen detecteren. Tevens laat ik zien hoe vaste-stof nanoporiën (net als de echte kernporie) bepaalde biologische moleculen kunnen selecteren voor transport, tenminste, wanneer we de porie bekleden met FG-Nup eiwitten. Dit hoofdstuk sluit ik vervolgens af met een beschrijving van de basisprincipes van DNA origami, en een overzicht van belangrijke wetenschappelijke artike-

len die verschenen zijn op het gebied van DNA-origami nanoporiën.

In **Hoofdstuk 2** vergelijk ik vaste-stof nanoporiën met biologische nanoporiën, dat wil zeggen, ik vergelijk hun algemene karakteristieken en hun stroomruis. Ik begin met het identificeren van de verschillende oorzaken van hoogfrequente en laagfrequente ruis. Want hoewel de oorzaak van de hoogfrequente ruis in beide systemen hetzelfde is, namelijk dielectrische ruis en capacitieve ruis, verschilt de oorzaak van de laagfrequente ruis: bij vaste-stof nanoporiën is het vooral  $1/f$  ruis, terwijl het bij biologische nanoporiën vooral protonatieruis is. Vervolgens vergelijk ik de signaal/ruis verhouding (SRV) van verschillende nanoporiën tijdens het transport van korte homopolymeren. Op basis van literatuurgegevens en data van zowel ons eigen lab als die van andere labs blijkt dat  $\text{SiN}_x$  vaste-stof nanoporiën de hoogste SRV hebben ( $\sim 37$ ). Dit komt doordat er in dit systeem relatief weinig laagfrequente ruis is, maar juist een relatief hoge stroomsterkte en dus een sterker signaal. Daarbij moet overigens opgemerkt worden dat de SRV van de biologische nanoporie MspA sterk verhoogd kan worden ( $>160\times$ ) door een DNA-motor eiwit aan de ingang van deze nanoporie te plaatsen. Ik sluit dit hoofdstuk af met een overzicht van de beste methoden om zowel hoog- als laagfrequente stroomruis te onderdrukken in biologische- en vaste-stof nanoporiën.

Tot op de dag van vandaag is er één bron van stroomruis die nanoporie wetenschappers niet goed begrijpen: de zogenaamde  $1/f$  ruis. In **Hoofdstuk 3** karakteriseer ik het laagfrequente ruis-spectrum van vaste-stof nanoporiën, en zien we dat de grootte van de fluctuaties in  $1/f$  ruis afneemt bij grotere nanoporiën. Hoewel deze interessante observatie niet nieuw is, bestond er nog geen theoretisch model om dit fenomeen op een analytische manier te verklaren. In dit hoofdstuk laat ik zien dat de globale trends van dit fenomeen goed te verklaren zijn door ook rekening te houden met de bijdrage van de nanoporie-ingang aan de  $1/f$  ruis, hetgeen in eerdere modellen niet gedaan werd. Verder introduceren we twee verschillende ‘Hooge parameters’ om twee lokale mechanismen voor ionenfluctuaties te beschrijven, enerzijds aan het oppervlakte van de nanoporie, en anderzijds in de bulk en de ingang van de nanoporie. Ons uiteindelijke model werkt hierdoor goed voor nanoporiën van verschillende diameters, en vormt daarmee een veralgemenisering van het Hooge model voor vaste-stof nanoporiën.

**Hoofdstuk 4** geeft een breed overzicht van het nanoporiën onderzoeksgebied, met de nadruk op toepassing die verder gaan dan het traditionele sequencen van DNA of RNA moleculen. Door belangrijke bijdragen van nanoporiën in andere onderzoeksgebieden te benadrukken laten we zien hoe veelzijdig en hoe breed toepasbaar zowel biologische als vaste-stof nanoporiën kunnen zijn, en hoe ze daardoor kunnen bijdragen aan een breed scala van wetenschappelijke uitdagingen. De veelzijdigheid van nanoporiën is te danken aan tenminste drie parameters die gevarieerd kunnen worden, zoals de lengte en de diameter van de porie, en de ‘bekleding’ van het oppervlakte waardoor de interactie met andere moleculen aangepast kan worden. In dit overzichtshoofdstuk komen onder meer de volgende toepassingen aan de orde: proteomics met moleculaire resolutie, biopsie van biomarkers met moleculaire resolutie, het creëren van nanoreactoren voor polymeerchemie en het nabootsen van biologische poriën (zoals de kernporie) om een

betreffend biologische transport proces te bestuderen.

In **Hoofdstuk 5** borduren we voort op eerder biomimetisch werk waarin de kernporie werd nagebootst door vaste-stof nanoporiën te bekleden met gezuiverde FG-Nup eiwitten. Hier maken we echter geen gebruik meer van een uit de natuur afkomstige FG-Nup, maar van een synthetisch FG-Nup eiwit dat we zelf ontworpen hebben en 'NupX' noemen. Onze hypothese is dat we de het gedrag van de kernporie zouden moeten kunnen nabootsen door kunstmatige 'designer FG-Nup' eiwitten te ontwerpen die voldoen aan dezelfde bouwkundige principes als hun natuurlijke tegenhangers. Drie bouwkundige principes hebben we weten te achterhalen door de aminozuursequentie van de belangrijkste GLFG-Nups uit bakkersgist te analyseren: (i) een bi-modale verdeling van zowel geladen als plakkerige aminozuren, om precies te zijn: een plakkerig N-terminaal domein met weinig lading, en een niet-plakkerig C-terminaal domein met relatief veel lading; (ii) een herhaling van het 'FG' of het 'GLFG' motief met een onderliggende afstand van 5-20 aminozuren in het plakkerige gedeelte; en (iii) eiwitten die intrinsieke ongeordend zijn, dat wil zeggen dat ze geen vaste drie-dimensionale structuur hebben. Om de selectiviteit van ons designer eiwit NupX te onderzoeken hebben we een QCM-D chip (waarmee eiwit-eiwit interacties gemeten kunnen worden) ermee bekleed, en konden we aantonen dat de kernporie-transporter Kap95 op een vergelijkbare manier bindt aan NupX als aan een natuurlijke FG-Nup. Het controle eiwit BSA daarentegen (dat niet betrokken is bij kernporietransport) bindt noch aan NupX noch aan zijn natuurlijke tegenhanger. En toen we biomimetische nanoporiën bekledden met NupX zagen we dat Kap95 (in tegenstelling tot BSA) de stroom van ionen onderbreekt, hetgeen aantoont dat het inderdaad middels NupX getransporteerd kan worden. Door deze experimentele resultaten te combineren met computersimulaties van de conformatie en de domein lokalisatie van NupX hebben we een gedetailleerd microscopisch beeld kunnen krijgen van deze biomimetische nanoporie. Samengevat toont dit hoofdstuk dus aan dat kernporietransport in het laboratorium ook goed nagebootst kan worden met een rationeel ontworpen synthetisch eiwit.

In **Hoofdstuk 6** bestuderen we met biomimetische nanoporiën de interactie tussen de kernporie-transporter Kap95 en een natuurlijk FG-Nup eiwit, namelijk Nsp1. In eerdere studies is weliswaar de selectiviteit van Nsp1 voor Kap95 aangetoond, maar in dit hoofdstuk wordt er pas voor het eerst gekeken naar de concentratieafhankelijkheid van dit transport, teneinde onderscheid te kunnen maken tussen twee conflicterende theoretische modellen: het Kap-centrische- en het FG- centrische model. Wanneer we een oplossing met Kap95 over een met Nsp1 beklede vaste-stof nanoporie spoelden namen we een gestage afname in de ionenstroom waar, hetgeen erop duidt dat een gedeelte van de Kap95 populatie aan Nsp1 bindt met een hoge affiniteit. Daarnaast observeerden we bovenop die gestage afname in de ionenstroom vele korte blokkades (van milisecondes) die duiden op een tweede populatie van Kap95 moleculen die snel getransporteerd worden. Een analyse van de laagfrequente ruis, die bij biomimetische nanoporiën vooral gekenmerkt wordt door FG-Nup fluctuaties in de nanoporie, toonde aan dat de  $1/f$  ruis afnam bij toenemende Kap95 concentraties. Dit is in overeenstemming met een verwachte versteviging van het FG-Nup netwerk in de nanoporie, die veroorzaakt

wordt door de eerstgenoemde populatie van hoog-affinititeit gebonden Kap95 moleculen. We bevestigen onze nanoporieteit-metingen met QCM-D metingen, waar we ook een concentratie-afhankelijke toename van Kap95 in het Nsp1 netwerk waarnemen. Met andere woorden, uit verschillende metingen blijkt dat er zowel een langzame als een snelle Kap95 populatie is in het FG-Nup netwerk van de nanoporieteit, wat in overeenstemming is met voorspellingen van het zogeheten Kap-centrische model.

De zoektocht naar betere biomimetische kernporiën heeft wetenschappers naar DNA origami geleid, omdat dat ingezet kan worden als een drie-dimensionale ringvormige mal waaraan FG-Nup eiwitten op een gecontroleerde manier vastgemaakt kunnen worden. Tot nu toe was het echter niet mogelijk om de transporteigenschappen van FG-Nups binnenin zo'n origami mal te bestuderen. In **Hoofdstuk 7** beschrijven we een nieuw methode om relatief grote (30 nm) DNA origami-poriën in te bouwen in het membraan van een liposoom, oftewel een vetblaasje. Teneinde de hoge energiebarrière (om een dusdanig groot object in een membraan te krijgen) te omzeilen hebben we gebruik gemaakt van de methode 'cDICE'. Hiermee werden de DNA-origami poriën al in het membraan ingebouwd op het moment dat dit gevormd wordt vanuit een omgekeerde emulsie. We hebben vervolgens geverifieerd dat de DNA-origami inderdaad de verwachte poriën vormen door de influx van verschillende moleculen erdoorheen te meten. Hieruit bleek dat kleine (GFP van ~30 kDa) tot middelgrote moleculen (dextran van ~250 kDa) de DNA-origami porie gemakkelijk konden passeren, maar grotere dextran moleculen niet, precies zoals verwacht op basis van de porie diameter. Daarnaast hebben we het aantal DNA-origami poriën per liposoom gekwantificeerd door middel van FRAP experimenten, waaruit blijkt dat er honderden in één enkel liposoom ingebouwd kunnen worden. Samengevat tonen deze experimenten aan dat DNA-origami poriën zeer geschikt zijn als biomimetische kernporie om het transport van biologische moleculen over de kernmembraan te bestuderen.

In **Hoofdstuk 8** blik ik terug op de resultaten die in dit proefschrift beschreven zijn, en stel ik nieuwe projecten en ontwikkelingen voor die gevuld zouden kunnen worden om onopgeloste problemen te benaderen. Zo stel ik voor om FG-Nup eiwitten in meer detail te bestuderen door de aminozuur samenstelling van synthetische designer FG-Nups systematisch te variëren, en het effect daarvan te bepalen op selectiviteit en transport. Ook stel ik nieuwe experimenten voor waarmee we de interacties tussen Kap-eiwitten en FG-Nups beter zouden kunnen karakteriseren, en hoe we op basis van DNA-origami biomimetische kernporiën zouden kunnen maken die dichter in de buurt komen van de natuurlijke kernporie. Als allerlaatste zoom ik uit op het gehele onderzoeksgebied dat transport door de kernporie bestudeert, en geef ik mijn visie op openstaande thema's zoals (i) de fase-scheiding van FG-Nup eiwitten; (ii) het samenspel tussen FG-Nups en Kap-eiwitten; en (iii) de drie-dimensionale structuur van de kernporie. Ik ben ervan overtuigd dat we een bevredigend mechanistisch inzicht in dit transport proces kunnen krijgen wanneer we deze verschillende thema's gelijktijdig aanpakken.